MXene-Embedded Porous Carbon-Based Cu_2O Nanocomposites for Non-Enzymatic Glucose Sensors

DOI:
10.1021/acsomega.3c09659

Document Version
Final published version

Published in:
ACS Omega

ACS OMEGA

Open Access

http://pubs.acs.org/journal/acsodf

Article

MXene-Embedded Porous Carbon-Based Cu_2O Nanocomposites for Non-Enzymatic Glucose Sensors

Tami Selvi Gopal,[¶] Jaimson T. James,[¶] Bharath Gunaseelan,[¶] Karthikeyan Ramesh, Vimala Raghavan, Christina Josephine Malathi A, K. Amarnath, V. Ganesh Kumar, Sofia Jennifer Rajasekaran, Saravanan Pandiaraj, Muthumareeswaran MR, Sudhagar Pitchaimuthu, Chamil Abeykoon, Abdullah N. Alodhayb, and Andrews Nirmala Grace*

Cite This: https://doi.org/10.1021/acsomega.3c09659

Read Online

ACCESS | Metrics & More | Article Recommendations

ABSTRACT: This work explores the use of MXene-embedded porous carbon-based Cu_2O nanocomposite (Cu_2O/M/AC) as a sensing material for the electrochemical sensing of glucose. The composite was prepared using the coprecipitation method and further analyzed for its morphological and structural characteristics. The highly porous scaffold of activated (porous) carbon facilitated the incorporation of MXene and copper oxide inside the pores and also acted as a medium for charge transfer. In the Cu_2O/M/AC composite, MXene and Cu_2O influence the sensing parameters, which were confirmed using electrochemical techniques such as cyclic voltammetry, electrochemical impedance spectroscopy, and amperometric analysis. The prepared composite shows two sets of linear ranges for glucose with a limit of detection (LOD) of 1.96 μM. The linear range was found to be 0.004 to 13.3 mM and 15.3 to 28.4 mM, with sensitivity values of 430.3 and 240.5 μA mM^{-1} cm^{-2}, respectively. These materials suggest that the prepared Cu_2O/M/AC nanocomposite can be utilized as a sensing material for non-enzymatic glucose sensors.

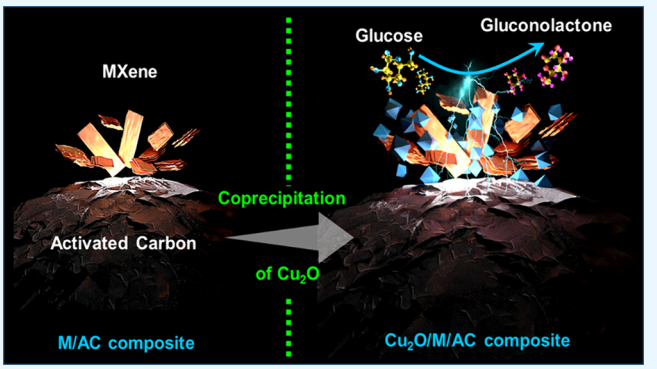

INTRODUCTION

The booming growth of biosensors in the market and its constant requirements for improving accuracy, stability, simplicity, miniaturization, powering aids, connectivity to smart devices, and scalability still serve as fuels in biosensor research. Worldwide, the growing sensor market must meet the needs of the population with diabetic complaint; an estimate of more than 600 million is projected by 2040 and, hence, the sensor should meet critical requirements such as frequent blood and/or glucose monitoring for effective diabetes management.[1] Electrochemical sensors perform well among the other methods in terms of efficiency, cost, accuracy, reliability, sensitivity, stability, and robustness.[2−4] The different steps of electrochemical biosensors are recognition, electrochemical transduction, signal processing, amplification, and data representation.[3,5] Based on the sensor recognizers, it can be categorized into enzymatic and nonenzymatic methods. In electrochemical glucose sensing using the enzymatic method, glucose in blood reacts with an enzyme, which is adhered to the recognizer, and the current across the electrode undergoes a variation and facilitates quantification of the level of glucose in the blood.[4,6] Although enzymatic sensors provide high selectivity and lesser response time, their single use and limited shelf life limit their wide and common usage as glucose sensors. On the contrary, non-enzymatic glucose sensors make use of inorganic catalysts, which gives it longer shelf life and reusability.[4] Non-enzymatic glucose sensors using Cu_2O, ZnO, MnO_2, CuO, and NiO nanomaterials had been developed and extensively studied as electrode materials.[6−9] Among them, Cu metal nanoparticles[10,11] and their oxides[12−15] have attracted significant attention due to their low cost, variety in morphologies, large specific surface area, excellent electrocatalytic activity, and easy electron transfer reactions at lower overpotentials. With these advantages, cuprous oxide (Cu_2O) has attracted significant interest as electrode material for electrochemical sensor fabrication, which has a band gap of 2.17 eV.[16−18] Yet, Cu_2O alone will not give high performance due to less sensitivity toward glucose oxidation, a small linear

Received: December 4, 2023
Revised: January 25, 2024
Accepted: January 31, 2024

range of detection, and poor conductivity.[16] In this regard, a supporting scaffold that can provide a wider spread and better surface area exposure for Cu_2O had to be considered. Over the past few years, scientists have noticed increased signaling in glucose sensing with the use of activated carbon (AC) as support material attributed to its large surface area, porosity, and surface chemical state. Being a cost-effective material with a simple synthesis procedure, AC's ability to conduct electrons to anode makes it a suitable material for sensing applications even for large-scale usage.[19]

The performance of a sensor is influenced by nanomaterials with varied sizes, shapes, and crystal facets. In contrast to a nanoparticle of larger size, the action of atoms at the corners and edges of nanoparticles becomes prominent as their sizes increase and thus exhibit intrinsically different catalytic performance.[20] In this case, materials with varied forms, such as sheets (2D materials), typically display quite different catalytic behavior that is essentially caused by variations in the geometric structure and electronic state of atoms on the surface.[21] Hence, for developing sensitive sensing platforms, 2D materials like graphene and molybdenum disulfide (MoS_2) have been researched intensively. But these materials have a few limitations, like challenges in surface functionalization and hydrophobicity. As a newcomer into the family of 2D materials, MXenes have already achieved much attention and have found their way into applications in the fields of electrochemical sensors, energy storage, energy conversion, EMI shielding, and more;[22−24] especially, MXenes like $Ti_3C_2T_x$ have shown more sensitivity in sensing bacteria, hydrogen peroxide, proteins, glucose, etc., than other 2D materials like graphene. While the lower performance of graphene has much to do with its hydrophobicity and lower electrical conductivity, MXenes are blessed with a hydrophilic surface (due to −OH, =O, and −F surface termination groups) and metal-like conductivity.[25] Along with some more traits such as increased surface area, direct charge transfer, and redox capability of MXenes, few studies on glucose sensors using MXene-based composites as a sensing element have been reported.

In 2016, Rakhil et al. reported an amperometry-based glucose biosensor that leverages the synergistic effect of the biosensing actions of MXene and Au nanoparticles. The device was tested with a linear amperometric response from 0.1 to 18 mM of glucose with a higher sensitivity of 4.2 μA mM^{-1} cm^{-2} and a LOD of 5.9 μM.[20] Recently, Manoj et al. synthesized free-standing, flexible electrodes for glucose sensing where the catalytically active cobalt oxide nanocubes were grown on MXene, which synergistically contributed to superior sensing performance. The device showed a linear range of 0.05 μM to 7.44 mM with a sensitivity of 19.3 μA mM^{-1} cm^{-2}.[25] A wearable non-invasive and nonenzymatic glucose sensor was fabricated by Li et al. by hybridizing Pt nanoparticles onto MXene nanosheets with a linear range of 0−8 mM and a LOD of 29.25 μM.[26] Another MXene-based enzymatic glucose sensor with 3D porous $Ti_3C_2T_x$ MXene/graphene/AuNPs (MGA) was fabricated by Feng's group. They explained that the $Ti_3C_2T_x$ nanosheets possess numerous hydrophilic groups, which make the composite hydrophilic in character. Hence, the porous composite has a more open structure and encourages the enzyme (glucose oxidase) to enter the pores, which may improve immobilization and retention of enzyme in the film.[27] Hence, these works show that MXenes can work as excellent sensing materials when composited with other materials synergistically for superior sensing of glucose.

In this work, a composite material of MXene-embedded porous carbon-based Cu_2O nanocomposite (Cu_2O/M/AC) is synthesized by the coprecipitation method and utilized as a sensor probe for glucose sensing. The prepared material was characterized by techniques such as FESEM, XRD, and electrochemical investigations like chronoamperometry (CA), which suggested that the material has a wide linear range with high sensitivity and good selectivity toward glucose sensing.

EXPERIMENTAL SECTION

Chemicals and Materials. Ti_3AlC_2 MAX powder, ethanol, deionized water (DIW), dimethyl sulfoxide (DMSO), glucose, copper chloride, and HF (40 wt %) were purchased from Sigma-Aldrich and used as received without any further purification. The etching process of the MAX phase, synthesis of activated carbon, and the composites of Cu_2O/MXene/activated carbon composites are shown schematically in Scheme 1.

Scheme 1. Schematic of the Synthesis Process of the Cu_2O/M/AC Composite

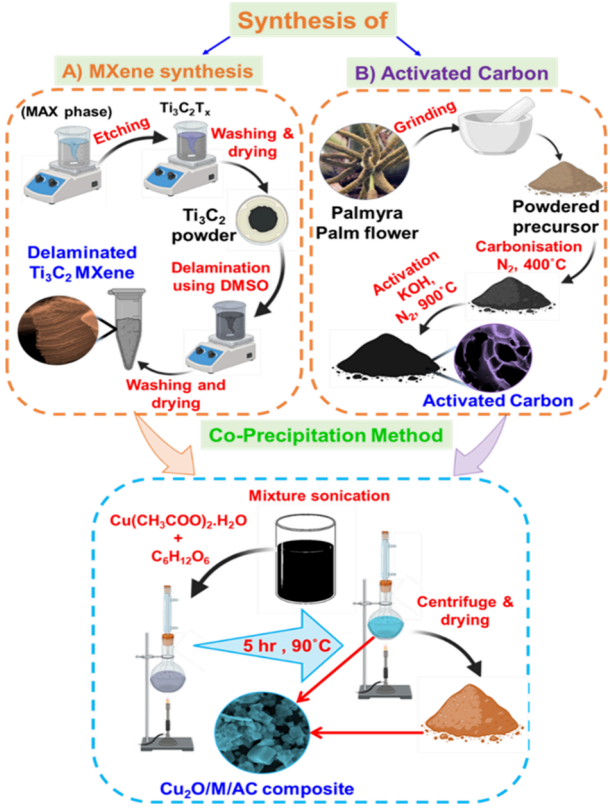

Synthesis of MXene. The etching of the MAX phase was carried out by the HF etching process, and the connection reaction is given in eq 1.[28−30]

$$Ti_3AlC_2(s) + 3HF(l) \rightarrow Ti_3C_2T_x(s) + AlF_3(s) + H_2O(l) + H(g)\uparrow \quad (1)$$

Under stirring conditions, 2 g of Ti_3AlC_2 MAX phase was slowly added into 50 mL of HF solution and then stirred for 48 h at 250 rpm, and the complete reaction was carried out at

https://doi.org/10.1021/acsomega.3c09659
ACS Omega XXXX, XXX, XXX−XXX

room temperature. After 48 h, the obtained black solution was washed in deionized water (DI) until the pH of the supernatant reaches to ~6.[31] The visual appearance of black sediment assumes the formation of multilayered MXene flakes as per eq 1. Further, multilayered MXene sheets were delaminated using dimethyl sulfoxide (DMSO) as an intercalating agent. In 25 mL of DMSO, 500 mg of etched MXene was added and then stirred for 18 h at room temperature. After this, the converted final product was washed several times with DI water and dried at 60 °C for 24 h.[32−35]

Synthesis of Activated Carbon or Porous Carbon (AC). Palmyra palm flower was chosen as a carbon source for synthesizing activated carbon. The dried palmyra palm flowers were ground into fine powder and carbonized by heating at 400 °C with a ramping of 5 °C min^{-1} in a N_2 environment. After carbonization, a 1:1 weight ratio of potassium hydroxide and carbonized palmyra palm flower sample was mixed together and heated at 900 °C for 1 h in a N_2 atmosphere. After this process, the pH of the obtained activated material was reduced to ~6 by adding HCl (30 wt %) and washing with DI water several times. After neutralization, the formed activated carbon was dried in an oven at 60 °C for 12 h.[36,37]

Synthesis of the MXene-Activated Carbon (AC) Composite (M-AC). The M-AC composite was prepared using an ultrasonication process. One hundred milligrams of MXene in 50 mL of DI water (solution-1) and 50 mg of activated carbon in 50 mL of DI water (solution-2) were sonicated for 30 min. The evenly dispersed MXene (solution-1) and AC (solution-2) solutions were mixed together and further sonicated for 1 h to form the M-AC composite. The composite solution formed was centrifuged and vacuum-dried at room temperature.

Synthesis of the Cu_2O/M/AC Composite. The prepared M-AC composite was combined with Cu_2O by the coprecipitation method. Initially, 100 mg of M-AC composite was dispersed in 100 mL of DI water via sonication, and then 1 g of copper acetate monohydrate ($Cu(CH_3COO)_2{\cdot}H_2O$) and 1.8 g of glucose ($C_6H_{12}O_6$) was added into the solution. The obtained solution was refluxed for 5 h at 90 °C. The formed precipitate was allowed to cool to room temperature and centrifuged. The settled precipitate was further washed in ethanol and dried in an oven for 12 h at 50 °C.[35,38−40] Similarly, bare Cu_2O and AC-Cu_2O composites were prepared without M-AC and with AC, respectively.

Material Characterizations and Electrochemical Measurements. X-ray diffraction of prepared composites was carried out with Bruker equipment (D8 Advance, CuKα radiation (λ = 1.54 Å)) to find the crystalline structure. The surface topography and elemental composition of the composite were confirmed by using FE-SEM (Carl Zeiss Model). Cyclic voltammetry (CV), electrochemical impedance spectroscopy (EIS), and chronoamperometry (CA) were studied using a CHI-660C workstation. In a three-electrode system, the Pt wire, Ag/AgCl, and modified glassy carbon electrode was used as a counter electrode, reference electrode, and working electrode, respectively. The sensing study was carried out in a 0.1 M NaOH solution. The preparation of the working electrode was carried out using the following steps. The glassy carbon electrode was initially polished with 1, 0.3, and 0.05 μm-sized alumina powder (Al_2O_3). After each polishing, the electrode was sonicated in ethanol and DI water, and then the electrode was dried under N_2 gas. MXene-activated carbon or Cu_2O/M/AC (1.5 mg) ink was prepared by sonicating the material in 250 μL of DI water and 5 μL of Nafion. After this, the suspension (5 μL) was coated on the polished GCE and dried for 12 h. After coating the prepared materials, the electrochemical studies were carried out with two electrolytes, viz., 0.1 M KCl and 5 mM $K_3[Fe(CN)_6]^{3-/4-}$ and 0.1 M NaOH. The ferri/ferrocyanide solution was used for studying the electrochemical properties of the coated electrodes, and then glucose sensing performance studies were carried out in a 0.1 M NaOH solution.

RESULTS AND DISCUSSION

Microscopic analysis was used to study the morphologies of the prepared materials systematically. The FESEM image (Figure 1A) confirms that the potassium hydroxide-treated and

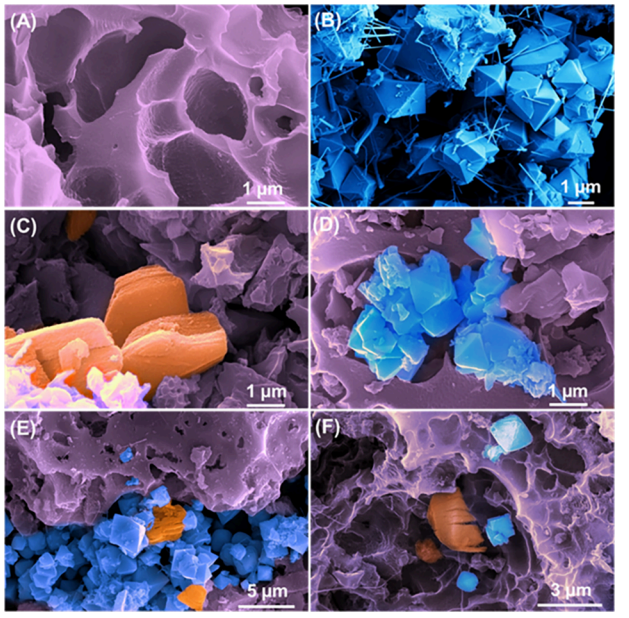

Figure 1. FESEM images of (A) activated carbon, (B) octahedral Cu_2O, (C) M-AC composite, (D) AC-Cu_2O composite, and (E, F) Cu_2O/M/AC composite (where MXene and Cu_2O are highlighted in brown and blue, respectively).

nitrogen atmospheric activated biomass-derived carbon exhibited more porosity at 6.758 μm, which was randomly distributed all over the surface.[41] When the activated carbon and MXene were sonicated, accordion-like MXene sheets were embedded in the pores of activated carbon, as given in Figure 1C, which would enhance the electron transfer rate during the oxidation of glucose.[42,43] To improve the catalytic activity of the glucose sensor, the Cu_2O nanoparticle was combined with the M-AC composite via a coprecipitation method. The formed ternary composite (Cu_2O/M/AC) (Figure 1E,F) shows octahedral-shaped Cu_2O anchored into the porous network, alike the morphology of bare Cu_2O octahedrons given in Figure 1B.[35] Cu_2O particles were seen to be distributed on the surfaces of MXene and activated carbon. The accordion structure of MXene in the ternary composite was retained as observed in the binary composite. For the bare Cu_2O metal oxide, both the octahedral particles and nanowires coexisted in this product, which might be due to the variation in the surface energies or else the growth rate variation of each face of Cu_2O as compared to the growth of Cu_2O in the ternary composite.[44] Further, the elemental composition of the

https://doi.org/10.1021/acsomega.3c09659
ACS Omega XXXX, XXX, XXX−XXX

ternary composite was confirmed using EDAX spectra and mapping analysis. The spectrum of the Cu_2O/M/AC composite is given in Figure 2A, which contains a 71.3%

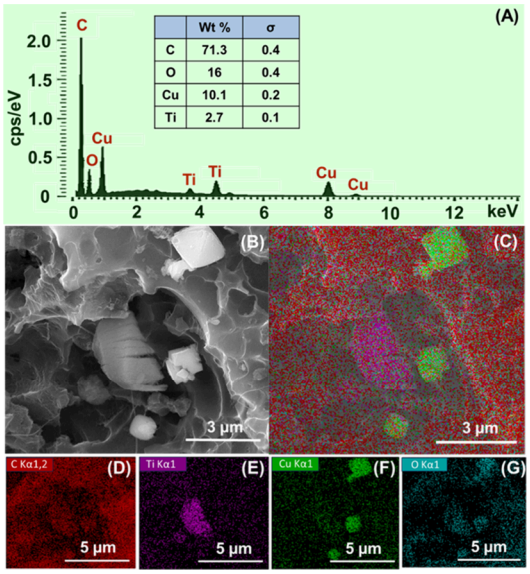

Figure 2. (A) EDAX spectrum of the Cu_2O/M/AC composite, (B) FESEM image of the Cu_2O/M/AC composite, (C) net EDAX mapping of the Cu_2O/M/AC composite, and (D−G) EDAX elemental mapping of carbon, titanium, copper, and oxygen present in the composite.

weight percentage of carbon, 16% weight percentage of oxygen, 10.1% weight percentage of Cu, and 2.7% weight percentage of titanium. The distribution of these elements is given in Figure 2C−G.

Thus, a homogeneous distribution of carbon elements with other elements such as copper, titanium, and oxygen confirms the formation of the Cu_2O/M/AC composite. The brightness of purple, green, and azure colors in EDAX mapping represents the higher concentration of Ti, Cu, and O elements, respectively. In the porous surface of activated carbon, two different shapes, viz., accordion and octahedrons, were observed. The accordion shapes were rich in Ti (Figure 2E), and the octahedral shapes were rich in Cu (Figure 2F) and O (Figure 2G). It suggests that the accordion shapes consist of $Ti_3C_2T_x$, and octahedron shapes were composed of micrometer-sized Cu_2O particles in the composites. Other than this, the mien of green (Figure 2F) and azure blue colors (Figure 2G) on the surface confirms the distribution of smaller-sized Cu_2O particles. Such structures are beneficial by providing more active sites for glucose oxidation.

Further, a Brunauer, Emmett, and Teller (BET) study of the synthesized bare materials and composites was conducted to determine their surface area. The BET analysis shows a surface area in the order of AC (950 $m^2 g^{-1}$) > Cu_2O/M/AC (11.3 $m^2 g^{-1}$) > MXene (6.533 $m^2 g^{-1}$). It exhibits reduced surface area for the Cu_2O/M/AC composite as compared with the palmyra palm flower-based activated carbon. It might be due to the fact that the Cu_2O particles were growing in the micropores as well as the presence of MXene in pores of activated carbon.[45] This finding was also seen in FESEM of the Cu_2O/M/AC composite. This deposition of metal oxides in the pores will enhance the active sites of the glucose sensor catalyst.

To know the crystalline structure and size of Cu_2O in the composites, XRD of bare Cu_2O, Cu_2O/AC, and Cu_2O/M/AC was performed, and it is given in Figure 3. The peaks appearing at 2θ values of 29.7° (110), 36.8° (111), 42.3° (200), 61.3° (220), and 73.5° (311) belong to cubic Cu_2O and well match with JCPDS card no. 05-0667.[46,47]

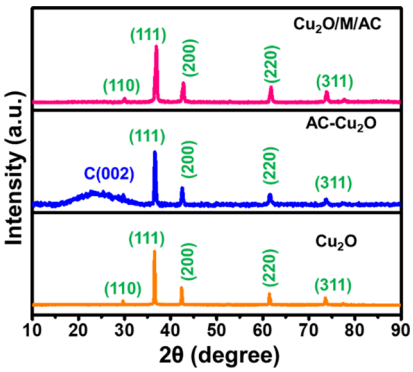

Figure 3. X-ray diffraction of Cu_2O, AC-Cu_2O, and Cu_2O/M/AC composites.

Along with Cu_2O peaks, a broad peak at 26° (002) confirms the formation of an activated carbon-based metal oxide composite. Even for the Cu_2O/M/AC ternary composite, crystalline peaks of Cu_2O appear in the XRD images, which is also evident in EDAX mapping. The order of cubic Cu_2O crystalline size is calculated to be Cu_2O/M/AC (18 nm) < Cu_2O-AC (22.1 nm) < bare Cu_2O (39 nm).

To understand the fundamental electron transfer process of the modified electrode, a combination of CV and EIS studies was carried out in a potassium ferri/ferrocyanide solution. Nyquist plots of AC-Cu_2O and MXene-combined AC-Cu_2O composite are given in Figure 4A. It displays a semicircle at high frequencies, which corresponds to the charge transfer resistance of the coated electrode.

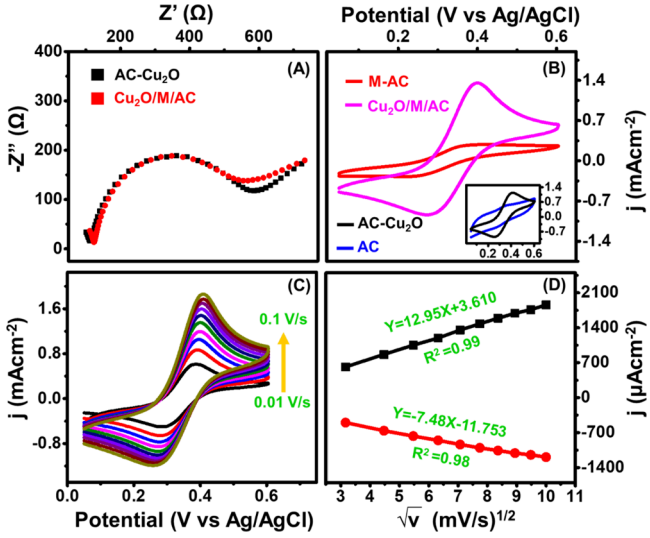

Figure 4. (A) Nyquist plots of composites, (B) CV of AC, AC-Cu_2O, M-AC, and Cu_2O/M/AC in a ferri/ferrocyanide electrolyte, (C) CV of Cu_2O/M/AC at different scan rates (0.01 to 0.1 V/s), and (D) plot of anodic and cathodic peak currents with respect to the square root of scan rates.

https://doi.org/10.1021/acsomega.3c09659
ACS Omega XXXX, XXX, XXX−XXX

The Cu_2O/M/AC composite (R_{ct} = 420 ohm/cm^2) shows the lowest charge transfer resistance as compared to the AC-Cu_2O composite (R_{ct} = 474 ohm/cm^2). It was able to speed up electron transfer on the testing electrode's surface when MXene was mixed with the AC-Cu_2O composite; this shows the strong electrostatic interaction between the changed electrode and the electrolytes.

Further, the half-wave potential (ΔE_{vp}) and peak current of the composite are given in the inset of Figure 4B. The order of ΔE_{vp} for the composites was Cu_2O/M/AC (112 mV/s) < Cu_2O/AC (148 mV/s). The lowest ΔE_{vp} and highest peak current of the prepared ternary composite indicate the adherence of MXene in the pores of AC, which might enhance the electrochemically active surface area and facilitate faster electron transfer between the electrode interface and the redox probe compared to Cu_2O/AC composites. Therefore, the prepared ternary composite will have a faster electron transfer ability between the coated electrode and the electrolyte while sensing the analyte.

Furthermore, a scan rate study was carried out, and it is shown in Figure 4C. As the scan rate increases, the current also increases; the measured current was plotted against the square root of the scan rate, which displays a linear increment (Figure 4D). It represents that the electrochemical reaction of glucose is a diffusion-controlled process for the MXene-adhered Cu_2O/AC composite electrode.

Based on the results of the ferri/ferrocyanide study, a comparative CV study of activated carbon and their composites in the absence and presence of glucose was carried out to investigate the effect of MXene adherence on the porous structure of activated carbon without and with Cu_2O (Figure 5).

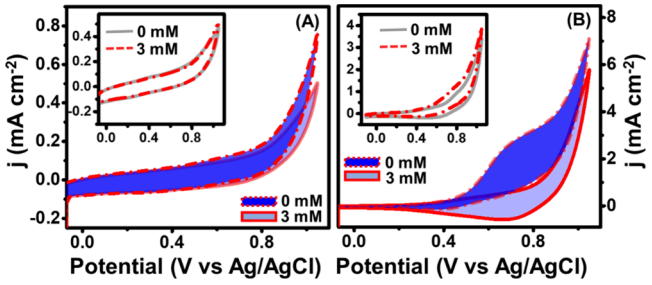

Figure 5. Sensing response study of different catalysts in the absence and presence of glucose: (A) M-AC and (B) Cu_2O/M/AC (insets of (A) AC and (B) AC-Cu_2O).

As shown in Figure 5A, the MXene/AC-modified electrode exhibits higher peak current as compared to the AC-based electrode (inset of Figure 5A) in the presence of glucose. In the case of the Cu_2O/M/AC composite, a high anodic shoulder peak current was observed within the potential window of 0.55 to 0.75 V during the addition of 3 mM glucose, which was higher than that of the AC-Cu_2O composite (Figure 5B and inset). The highest anodic shoulder peak was assumed to be due to glucose oxidation as per the sensing mechanism of the Incipient Hydrous Oxide Adatom Mediator (IHOAM) model.[48]

These good responses show the existence of more active sites on a working electrode surface for glucose molecule adsorption and oxidation. The combined properties of the M-AC composite, such as hydrophilicity, high conductivity, and large surface area of MXene,[25] along with the porous structure of activated carbon, enhance the formation of Cu_2O nanoparticles on the surfaces of the composite due to the overall synergistic effect and overall property of the composite. Thus, the formed heterostructure facilitates faster electron transfer between the interface of electrode and electrolyte during glucose oxidation.

Further, to understand the effect of the electrolyte, an optimization of electrolyte concentration for achieving the high sensitivity of the Cu_2O/MXene/AC composite was carried out by CV using different concentrations of NaOH (C_{NaOH}) from 0.05 to 0.2 M. From Figure 6A–D, the maximum change in

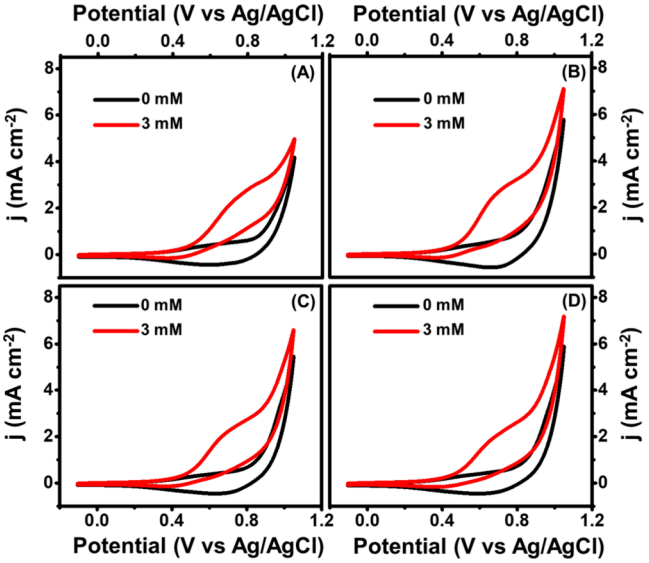

Figure 6. Electrolyte concentration optimization for the Cu_2O/M/AC composite with different molarity of NaOH: (A) 0.05, (B) 0.10, (C) 0.15, and (D) 0.20 M.

the oxidation current in the presence of glucose was achieved when C_{NaOH} was 0.1 M as compared to other concentrations. From the optimization results, 0.1 M NaOH was used for studying the sensing performance of the prepared Cu_2O/MXene/AC composite. The CV response of the prepared Cu_2O/M/AC composite at different glucose concentrations was studied, and the change in current is given in Figure 7A.

Generally, the sensor's amperometric performance toward the analyte depends on the operating potential. An optimized operating potential was found by varying the applied bias to observe the best amperometric performance. In Figure 7B, operating potentials of 0.55, 0.60, 0.65, and 0.70 V show a step-like current response with successive addition of 0.1 mM

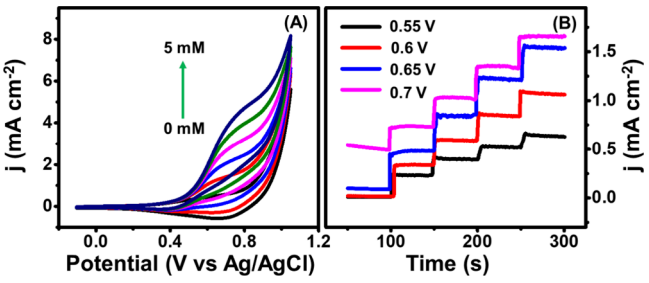

Figure 7. (A) Cyclic voltammetry study of the Cu_2O/M/AC composite at different concentrations of glucose (0–5 mM) and (B) potential optimization for the Cu_2O/M/AC composite.

https://doi.org/10.1021/acsomega.3c09659
ACS Omega XXXX, XXX, XXX−XXX

glucose. A stepwise enhancement of current with respect to glucose addition at 0.65 V was observed in comparison to the higher and lower applied bias. Hence, to find the limit of detection (LOD) and sensitivity, amperometric sensing of glucose was carried out using the same optimized potential (0.65 V).

With the optimized electrolyte concentration and potential, the amperometric performance of the Cu_2O/M/AC composite was carried out with the successive addition of glucose with increasing concentrations under stirring conditions. It can be observed (Figure 8A) that the composite material responds

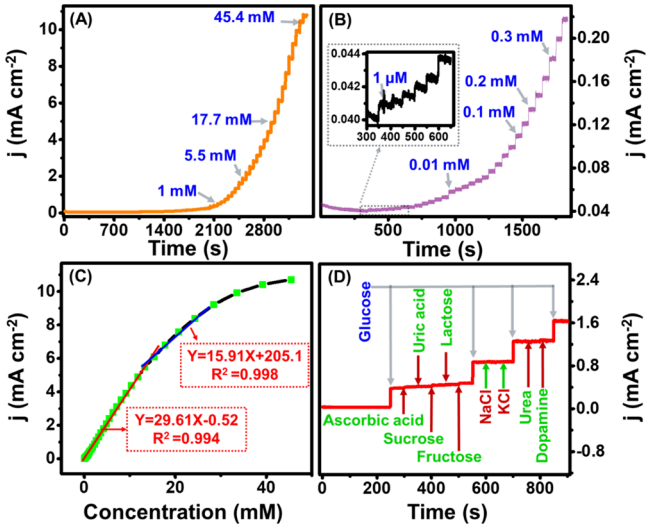

Figure 8. Sensing performance study of the Cu_2O/M/AC composite. (A) Amperometric response, (B) expanded view of lower concentrations, (C) linear fitting curve of glucose concentration vs current, and (D) selectivity study using 1 mM glucose concentration along with 0.1 mM of other analytes (inset of panel B is the amperometric response in 1 μM glucose concentration).

immediately to the addition of glucose starting from 1 μM (inset of Figure 8B). Before the subsequent addition of glucose, the current reaches a steady state after three seconds, representing the formation of gluconolactone due to the fast electrocatalytic activity of the composite material.[46] After each addition of glucose, the system again reached a steady state. An expanded view of current variations due to lower concentrations of glucose is shown in Figure 8B. This indicates that the composite was capable of a feeble current response to 1 μM analyte also. From the chronoamperometric study, a plot with glucose concentration against current response gives the calibration plot (Figure 8C) for finding the sensing parameters such as sensitivity, limit of detection, and linear range of detection of the prepared composite. The plot shows linear behavior at two linear regions. The linear range of 0.004 mM to 13.3 mM (LOD of 1.96 μM) and 15.3 mM to 28.4 mM (LOD of 7.91 mM), the corresponding regression equation obtained by fitting is given as I_p= 29.61X −0.520 (R^2 = 0.994) and I_p= 15.91X + 205.10 (R^2=0.998). The sensitivity of the electrode was found to be 430.3 $\mu AmM^{-1}cm^{-2}$ and 240.5 $\mu AmM^{-1}cm^{-2}$ with a low limit of detection of 1.96 μM. A comparative sensing performance of the prepared Cu_2O/M/AC composite with the other materials reported in the literature is tabulated in Table 1. It shows that the formed MXene embedded porous carbon based Cu_2O composite offers a wide linear range with good sensitivity and selectivity.

Table 1. Comparative Sensing Performance of the Cu_2O/M/AC Composite with the Other Sensing Elements Reported in the Literature*

electrode material	linear range (mM)	detection limit (μM)	sensitivity ($\mu A\ cm^{-2}\ mM^{-1}$)	reference
Cu/Cu_2O nanoclusters	0.01−0.690	5	63.8	49
	1.190−3.69		22.6	
Co_3O_4/CuO nanorod array	0.001−0.5	0.38	5405	50
Cu_2O/Cu/CC	0.001−1.5	0.06	6952	51
Cu_2O MSs/S-MWCNT	0.00495−7	1.46	581.89	52
CuCNA/CF	0.2−1900	0.04	3826	53
GO_x-Pt-PAA-SPCE	0.02−2.3	7.6	42.7	54
GO_x-AC-$NiFe_2O_4$/CPE	2−10	0.001	32.01	55
AuNi@AC	0−1.7	0.41	1955	56
GrGO/AC	0.002−10	2	61.06	57
CuO/NiO/ACF	0.00025−5	0.146	247	58
Ti_2C-TiO_2	0.0001−0.2	0.12	75.32	59
Ti_3C_2-aUV	0.1−10	12.1	93.75	60
Cu_2O/M/AC	**0.004−13.3**	**1.96**	**430.3**	**This work**
	15.3−28.4		**240.5**	

*AC-activated carbon, SPCE-screen printed carbon electrode, ACF-Activated carbon nanofiber, CPE-Carbon Paste electrode.

To understand about the selectivity of Cu_2O/AC/M composite toward the desired analyte, i.e., glucose, current response was measured in the presence of other compounds that can possibly be present in the blood composition, such as ascorbic acid, sucrose, fructose, lactose, uric acid, NaCl, KCl, urea, and dopamine. Figure 8D shows a good selectivity of the electrode material toward glucose, where a prominent change in the current response is observed with the addition of glucose. The high selectivity of the material toward glucose could be due to the ability of the composite present in the electrode to oxidize the glucose molecule selectively, which in turn gives out an electron and, thus an increased current.[61]

The analysis of glucose in the presence of human serum sample for the prepared composite using the amperometric method is done to understand the real time compatibility of prepared composite. To carry out this, a blood sample was collected from healthy persons, and then a separation of the serum sample was carried out. Under stirring conditions, 100 μL of the separated serum was added into the electrolyte, followed by spiking of known glucose concentration, and then the variation of current was observed. Likewise, this procedure was repeated for one more serum sample. The glucose concentration was tabulated (Table 2), and from the table, it could be observed that the found glucose concentrations were of 99% recovery value from the spiked concentration. This indicates that the prepared Cu_2O/M/AC composite electrode was also suitable for real-time applications, as well.

Table 2. A comparison of the spiked and found glucose concentrations for the prepared composite electrode

Sample	Spiked glucose concentration (mM)	Obtained glucose concentration (mM)	Recovery (%)
Serum 1	3.1 mM	3.07 mM	99.1
Serum-2	2 mM	1.97 mM	99

https://doi.org/10.1021/acsomega.3c09659
ACS Omega XXXX, XXX, XXX−XXX

CONCLUSIONS

MXene embedded porous carbon based Cu_2O nanocomposite (Cu_2O/M/AC) shows a wide linear range for nonenzymatic glucose sensor with good selectivity and sensitivity. The material formation and morphology of the prepared composite show the presence of embedded MXene and Cu_2O in the pores of the activated carbon, and the metal oxides were seen distributed on the surface of the composites. The composite electrode exhibits a sensitivity of 430.3 $\mu AmM^{-1}cm^{-2}$ (0.004 mM to 13.3 mM) and 240.5 $\mu AmM^{-1}cm^{-2}$ (15.3 mM to 28.4 mM), respectively with a good selectivity and a low limit of detection viz. 1.96 μM. The prepared Cu_2O/M/AC composite was also found suitable for real-time analysis of serum samples with a recovery of 99%. With these features, the formed composite can serve well as a sensing element for nonenzymatic glucose sensor.

AUTHOR INFORMATION

Corresponding Author

Andrews Nirmala Grace − *Centre for Nanotechnology Research, Vellore Institute of Technology, Vellore, Tamil Nadu 632014, India;* orcid.org/0000-0002-2016-3013; Email: anirmalaglady s@gmail.com

Authors

Tami Selvi Gopal − *Centre for Nanotechnology Research, Vellore Institute of Technology, Vellore, Tamil Nadu 632014, India*

Jaimson T. James − *Centre for Nanotechnology Research, Vellore Institute of Technology, Vellore, Tamil Nadu 632014, India*

Bharath Gunaseelan − *Centre for Nanotechnology Research, Vellore Institute of Technology, Vellore, Tamil Nadu 632014, India*

Karthikeyan Ramesh − *Centre for Nanotechnology Research, Vellore Institute of Technology, Vellore, Tamil Nadu 632014, India*

Vimala Raghavan − *Centre for Nanotechnology Research, Vellore Institute of Technology, Vellore, Tamil Nadu 632014, India*

Christina Josephine Malathi A − *Department of Communication Engineering, School of Electronics Engineering (SENSE), Vellore Institute of Technology, Vellore, Tamil Nadu 632014, India*

K. Amarnath − *Department of Chemistry and Centre for Ocean Research, Sathyabama Institute of Science and Technology, Chennai 600119, India*

V. Ganesh Kumar − *Department of Chemistry and Centre for Ocean Research, Sathyabama Institute of Science and Technology, Chennai 600119, India*

Sofia Jennifer Rajasekaran − *Department of Physics, PPG Institute of Technology, Coimbatore 641034, India*

Saravanan Pandiaraj − *Department of Self-Development Skills, King Saud University, Riyadh 11451, Saudi Arabia*

Muthumareeswaran MR − *College of Science, King Saud University, Riyadh 11451, Saudi Arabia*

Sudhagar Pitchaimuthu − *Research Centre for Carbon Solutions, Institute of Mechanical, Processing and Energy Engineering, School of Engineering & Physical Sciences, Heriot-Watt University, Edinburgh EH14 4AS, U.K.;* orcid.org/0000-0001-9098-8806

Chamil Abeykoon − *Northwest Composites Centre, Aerospace Research Institute, and Department of Materials, Faculty of Science and Engineering, The University of Manchester, Manchester M13 9PL, U.K.;* orcid.org/0000-0002-6797-776X

Abdullah N. Alodhayb − *Department of Physics and Astronomy, College of Science, King Saud University, Riyadh 11451, Saudi Arabia;* orcid.org/0000-0003-0202-8712

Complete contact information is available at: https://pubs.acs.org/10.1021/acsomega.3c09659

Author Contributions

¶T.S.G., J.T.J., and B.G. contributed equally to this work.

Notes

The authors declare no competing financial interest.

ACKNOWLEDGMENTS

The authors extend their appreciation to the Deputyship for Research and Innovation, Ministry of Education in Saudi Arabia for funding this research work through the project no. (IFKSUOR3-099-8).

REFERENCES

(1) Dagogo-Jack, S. *Diabetes Mellitus in Developing Countries and Underserved Communities*. Springer Cham 2016, 1 294 .

(2) Xuan, X.; Yoon, H. S.; Park, J. Y. A Wearable Electrochemical Glucose Sensor Based on Simple and Low-Cost Fabrication Supported Micro-Patterned Reduced Graphene Oxide Nanocomposite Electrode on Flexible Substrate. *Biosens. Bioelectron.* **2018**, *109*, 75−82.

(3) Martinkova, P.; Pohanka, M. Biosensors for Blood Glucose and Diabetes Diagnosis: Evolution, Construction, and Current Status. *Anal. Lett.* **2015**, *48* (16), 2509−2532.

(4) Tian, K.; Prestgard, M.; Tiwari, A. A Review of Recent Advances in Nonenzymatic Glucose Sensors. *Mater. Sci. Eng., C* **2014**, *41*, 100−118.

(5) Chaiyo, S.; Mehmeti, E.; Siangproh, W.; Hoang, T. L.; Nguyen, H. P.; Chailapakul, O.; Kalcher, K. Non-Enzymatic Electrochemical Detection of Glucose with a Disposable Paper-Based Sensor Using a Cobalt Phthalocyanine−Ionic Liquid−Graphene Composite. *Biosens. Bioelectron.* **2018**, *102*, 113−120.

(6) Kim, S. E.; Yoon, J. C.; Tae, H.-J.; Muthurasu, A. Electrospun Manganese-Based Metal−Organic Frameworks for MnO_x Nanostructures Embedded in Carbon Nanofibers as a High-Performance Nonenzymatic Glucose Sensor. *ACS Omega* **2023**, *8* (45), 42689−42698.

(7) Zhu, H.; Li, L.; Zhou, W.; Shao, Z.; Chen, X. Advances in Non-Enzymatic Glucose Sensors Based on Metal Oxides. *J. Mater. Chem. B* **2016**, *4* (46), 7333−7349.

(8) Kaewsaenee, J.; Singhaset, M. T.; Roongraung, K.; Kemacheevakul, P.; Chuangchote, S. Polymer-Assisted Coprecipitation Synthesized Zinc Oxide Nanoparticles and Their Uses for Green Chemical Synthesis via Photocatalytic Glucose Conversions. *ACS Omega* **2023**, *8*, 43664−43673.

(9) Yang, Z.; Xu, W.; Yan, B.; Wu, B.; Ma, J.; Wang, X.; Qiao, B.; Tu, J.; Pei, H.; Chen, D.; Wu, Q. Gold and Platinum Nanoparticle-Functionalized TiO_2 Nanotubes for Photoelectrochemical Glucose Sensing. *ACS Omega* **2022**, *7* (2), 2474−2483.

(10) Kang, X.; Mai, Z.; Zou, X.; Cai, P.; Mo, J. A Sensitive Nonenzymatic Glucose Sensor in Alkaline Media with a Copper Nanocluster/Multiwall Carbon Nanotube-Modified Glassy Carbon Electrode. *Anal. Biochem.* **2007**, *363* (1), 143−150.

(11) Watanabe, T.; Ivandini, T. A.; Makide, Y.; Fujishima, A.; Einaga, Y. Selective Detection Method Derived from a Controlled Diffusion Process at Metal-Modified Diamond Electrodes. *Anal. Chem.* **2006**, *78* (22), 7857−7860.

https://doi.org/10.1021/acsomega.3c09659
ACS Omega XXXX, XXX, XXX−XXX

(12) Reitz, E.; Jia, W.; Gentile, M.; Wang, Y.; Lei, Y. CuO Nanospheres Based Nonenzymatic Glucose Sensor. *Electroanalysis* **2008**, *20* (22), 2482−2486.
(13) Zhuang, Z.; Su, X.; Yuan, H.; Sun, Q.; Xiao, D.; Choi, M. M. F. An Improved Sensitivity Non-Enzymatic Glucose Sensor Based on a CuO Nanowire Modified Cu Electrode. *Analyst* **2008**, *133* (1), 126−132.
(14) Kumar, S. A.; Cheng, H. W.; Chen, S. M.; Wang, S. F. Preparation and Characterization of Copper Nanoparticles/Zinc Oxide Composite Modified Electrode and Its Application to Glucose Sensing. *Mater. Sci. Eng., C* **2010**, *30* (1), 86−91.
(15) Wang, C.; Yin, L.; Zhang, L.; Gao, R. Ti/TiO_2 Nanotube Array/Ni Composite Electrodes for Nonenzymatic Amperometric Glucose Sensing. *J. Phys. Chem. C* **2010**, *114* (10), 4408−4413.
(16) Yazid, S. N. A. M.; Isa, I. M.; Hashim, N. Novel Alkaline-Reduced Cuprous Oxide/Graphene Nanocomposites for Non-Enzymatic Amperometric Glucose Sensor Application. *Mater. Sci. Eng., C* **2016**, *68*, 465−473.
(17) Lu, W.; Sun, Y.; Dai, H.; Ni, P.; Jiang, S.; Wang, Y.; Li, Z.; Li, Z. Direct Growth of Pod-like Cu_2O Nanowire Arrays on Copper Foam: Highly Sensitive and Efficient Nonenzymatic Glucose and H2O2 Biosensor. *Sensors Actuators, B Chem.* **2016**, *231*, 860−866.
(18) Khan, R.; Ahmad, R.; Rai, P.; Jang, L. W.; Yun, J. H.; Yu, Y. T.; Hahn, Y. B.; Lee, I. H. Glucose-Assisted Synthesis of Cu_2O Shuriken-like Nanostructures and Their Application as Nonenzymatic Glucose Biosensors. *Sensors Actuators, B Chem.* **2014**, *203*, 471−476.
(19) Li, T.; Ma, R.; Lin, J.; Hu, Y.; Zhang, P.; Sun, S.; Fang, L. The Synthesis and Performance Analysis of Various Biomass-Based Carbon Materials for Electric Double-Layer Capacitors: A Review. *Int. J. Energy Res.* **2020**, *44* (4), 2426−2454.
(20) Rakhi, R. B.; Nayak, P.; Xia, C.; Alshareef, H. N. Novel Amperometric Glucose Biosensor Based on MXene Nanocomposite. *Sci. Rep.* **2016**, *6*, 1−10.
(21) Vaghasiya, J. V.; Mayorga-Martinez, C. C.; Sofer, Z.; Pumera, M. MXene-Based Flexible Supercapacitors: Influence of an Organic Ionic Conductor Electrolyte on the Performance. *ACS Appl. Mater. Interfaces* **2020**, *12* (47), 53039−53048.
(22) Bian, R.; He, G.; Zhi, W.; Xiang, S.; Wang, T.; Cai, D. Ultralight MXene-Based Aerogels with High Electromagnetic Interference Shielding Performance. *J. Mater. Chem. C* **2019**, *7* (3), 474−478.
(23) Wang, C. H.; Kurra, N.; Alhabeb, M.; Chang, J. K.; Alshareef, H. N.; Gogotsi, Y. Titanium Carbide (MXene) as a Current Collector for Lithium-Ion Batteries. *ACS Omega* **2018**, *3* (10), 12489−12494.
(24) Kalambate, P. K.; Gadhari, N. S.; Li, X.; Rao, Z.; Navale, S. T.; Shen, Y.; Patil, V. R.; Huang, Y. Recent Advances in MXene−Based Electrochemical Sensors and Biosensors. *TrAC - Trends Anal. Chem.* **2019**, *120*, No. 115643.
(25) Manoj, D.; Aziz, A.; Muhammad, N.; Wang, Z.; Xiao, F.; Asif, M.; Sun, Y. Integrating Co3O4nanocubes on MXene Anchored CFE for Improved Electrocatalytic Activity: Freestanding Flexible Electrode for Glucose Sensing. *J. Environ. Chem. Eng.* **2022**, *10* (5), No. 108433.
(26) Li, Q. F.; Chen, X.; Wang, H.; Liu, M.; Peng, H. L. Pt/MXene-Based Flexible Wearable Non-Enzymatic Electrochemical Sensor for Continuous Glucose Detection in Sweat. *ACS Appl. Mater. Interfaces* **2022**, 13290 DOI: 10.1021/acsami.2c20543.
(27) Feng, L.; Qin, W.; Wang, Y.; Gu, C.; Li, X.; Chen, J.; Chen, J.; Qiao, H.; Yang, M.; Tian, Z.; Yin, S. $Ti_3C_2T_x$ MXene/Graphene/AuNPs 3D Porous Composites for High Sensitivity and Fast Response Glucose Biosensing. *Microchem. J.* **2023**, *184* (PA), No. 108142.
(28) Gu, H.; Xing, Y.; Xiong, P.; Tang, H.; Li, C.; Chen, S.; Zeng, R.; Han, K.; Shi, G. Three-Dimensional Porous $Ti_3C_2T_x$ MXene-Graphene Hybrid Films for Glucose Biosensing. *ACS Appl. Nano Mater.* **2019**, *2* (10), 6537−6545.
(29) Tang, Y.; Zhu, J.; Yang, C.; Wang, F. Enhanced Capacitive Performance Based on Diverse Layered Structure of Two-Dimensional Ti_3C_2 MXene with Long Etching Time. *J. Electrochem. Soc.* **2016**, *163* (9), A1975−A1982.
(30) Mashtalir, O.; Naguib, M.; Dyatkin, B.; Gogotsi, Y.; Barsoum, M. W. Kinetics of Aluminum Extraction from Ti_3AlC_2 in Hydrofluoric Acid. *Mater. Chem. Phys.* **2013**, *139* (1), 147−152.
(31) Wang, K.; Zhou, Y.; Xu, W.; Huang, D.; Wang, Z.; Hong, M. Fabrication and Thermal Stability of Two-Dimensional Carbide Ti_3C_2 Nanosheets. *Ceram. Int.* **2016**, *42* (7), 8419−8424.
(32) Thakur, A.; Chandran B.S, N.; Davidson, K.; Bedford, A.; Fang, H.; Im, Y.; Kanduri, V.; Wyatt, B. C.; Nemani, S. K.; Poliukhova, V.; Kumar, R.; Fakhraai, Z.; Anasori, B. Step-by-Step Guide for Synthesis and Delamination of $Ti_3C_2T_x$ MXene. *Small Methods* **2023**, *7* (8), e2300030 DOI: 10.1002/smtd.202300030.
(33) Kim, Y. J.; Kim, S. J.; Seo, D.; Chae, Y.; Anayee, M.; Lee, Y.; Gogotsi, Y.; Ahn, C. W.; Jung, H. T. Etching Mechanism of Monoatomic Aluminum Layers during MXene Synthesis. *Chem. Mater.* **2021**, *33* (16), 6346−6355.
(34) Alhabeb, M.; Maleski, K.; Anasori, B.; Lelyukh, P.; Clark, L.; Sin, S.; Gogotsi, Y. Guidelines for Synthesis and Processing of Two-Dimensional Titanium Carbide ($Ti_3C_2T_x$ MXene). *Chem. Mater.* **2017**, *29* (18), 7633−7644.
(35) Gopal, T. S.; Jeong, S. K.; Alrebdi, T. A.; Pandiaraj, S.; Alodhayb, A.; Muthuramamoorthy, M.; Grace, A. N. MXene-Based Composite Electrodes for Efficient Electrochemical Sensing of Glucose by Non-Enzymatic Method. *Mater. Today Chem.* **2022**, *24*, No. 100891.
(36) Raghavan, V.; Rajasekaran, S. J. Palmyra Palm Flower Biomass-Derived Activated Porous Carbon and Its Application as a Supercapacitor Electrode. *J. Electrochem. Sci. Eng.* **2022**, *12* (3), 545−556, DOI: 10.5599/jese.1314.
(37) Sivakumar Natarajan, T.; Bajaj, H. C.; Tayade, R. J. Palmyra Tuber Peel Derived Activated Carbon and Anatase TiO_2 Nanotube Based Nanocomposites with Enhanced Photocatalytic Performance in Rhodamine 6G Dye Degradation. *Process Saf. Environ. Prot.* **2016**, *104*, 346−357.
(38) Li, K.; Lei, Y.; Liao, J.; Zhang, Y. Facile Synthesis of MXene-Supported Copper Oxide Nanocomposites for Catalyzing the Decomposition of Ammonium Perchlorate. *Inorg. Chem. Front.* **2021**, *8* (7), 1747−1761.
(39) Gao, Y.; Wang, L.; Li, Z.; Zhou, A.; Hu, Q.; Cao, X. Preparation of MXene-Cu_2O Nanocomposite and Effect on Thermal Decomposition of Ammonium Perchlorate. *Solid State Sci.* **2014**, *35*, 62−65.
(40) Alanazi, N.; Selvi Gopal, T.; Muthuramamoorthy, M.; Alobaidi, A. A. E.; Alsaigh, R. A.; Aldosary, M. H.; Pandiaraj, S.; Almutairi, M.; Grace, A. N.; Alodhayb, A. Cu_2O/MXene/RGO Ternary Nanocomposites as Sensing Electrodes for Nonenzymatic Glucose Sensors. *ACS Appl. Nano Mater.* **2023**, *6* (13), 12271−12281.
(41) Goskula, S.; Siliveri, S.; Gujjula, S. R.; Chirra, S.; Adepu, A. K.; Narayanan, V. Sustainable Development of Activated Porous Carbon Materials from Gum Arabic Tree Seed Shell for CO_2 Capture. *Water. Air. Soil Pollut.* **2023**, *234* (8), 513 DOI: 10.1007/s11270-023-06529-9.
(42) Wang, L.; Liu, H.; Lv, X.; Cui, G.; Gu, G. Facile Synthesis 3D Porous MXene $Ti_3C_2T_x$@RGO Composite Aerogel with Excellent Dielectric Loss and Electromagnetic Wave Absorption. *J. Alloys Compd.* **2020**, *828*, No. 154251.
(43) Khan, R.; Andreescu, S. Mxenes-Based Bioanalytical Sensors: Design, Characterization, and Applications. *Sensors* **2020**, *20* (18), 1−19.
(44) Yang, Z.; Sun, S.; Kong, C.; Song, X.; Ding, B. Designated-Tailoring on {100} Facets of Cu2O Nanostructured From Octahedral to its Different Truncated Forms. *Journal of Nanomaterials.* **2010**, *2010*, 1−11.
(45) Hashem, B. Y.; Alswat, A. A.; Ali, S. L.; Al-Odaini, N. A.; Alshorifi, F. T. Facile synthesis of NiO-CuO/activated Carbon Nanocomposites for use in the Removal of Lead and Cadmium Ions from Water. ACS. *Omega.* **2022**, *7* (50), 47183−47191.
(46) Arifutzzaman, A.; Musa, I. N.; Aroua, M. K.; Saidur, R. MXene Based Activated Carbon Novel Nano-Sandwich for Efficient CO_2 adsorption in Fixed-Bed Column. *J. CO2 Util.* **2023**, *68* (October 2022), No. 102353.

https://doi.org/10.1021/acsomega.3c09659
ACS Omega XXXX, XXX, XXX−XXX

(47) Farooq, S.; Al Maani, A. H.; Naureen, Z.; Hussain, J.; Siddiqa, A.; Al Harrasi, A. Synthesis and Characterization of Copper Oxide-Loaded Activated Carbon Nanocomposite: Adsorption of Methylene Blue, Kinetic, Isotherm, and Thermodynamic Study. *J. Water Process Eng.* **2022**, *47* (March), No. 102692.
(48) Li, D. N.; He, Y. M.; Feng, J. J.; Zhang, Q. L.; Zhang, L.; Wu, L.; Wang, A. J. Facile Synthesis of Prickly Platinum-Palladium Core-Shell Nanocrystals and Their Boosted Electrocatalytic Activity towards Polyhydric Alcohols Oxidation and Hydrogen Evolution. *J. Colloid Interface Sci.* **2018**, *516*, 476−483.
(49) Yin, H.; Cui, Z.; Wang, L.; Nie, Q. In Situ Reduction of the Cu/Cu_2O/Carbon Spheres Composite for Enzymaticless Glucose Sensors. *Sensors Actuators, B Chem.* **2016**, *222*, 1018−1023.
(50) Cheng, S.; DelaCruz, S.; Chen, C.; Tang, Z.; Shi, T.; Carraro, C.; Maboudian, R. Hierarchical Co_3O_4/CuO Nanorod Array Supported on Carbon Cloth for Highly Sensitive Non-Enzymatic Glucose Biosensing. *Sensors Actuators, B Chem.* **2019**, *298* (July), No. 126860.
(51) Zhang, H.; Yu, Y.; Shen, X.; Hu, X. A Cu_2O/Cu/Carbon Cloth as a Binder-Free Electrode for Non-Enzymatic Glucose Sensors with High Performance. *New J. Chem.* **2020**, *44* (5), 1993−2000.
(52) Waqas, M.; Wu, L.; Tang, H.; Liu, C.; Fan, Y.; Jiang, Z.; Wang, X.; Zhong, J.; Chen, W. Cu_2O Microspheres Supported on Sulfur-Doped Carbon Nanotubes for Glucose Sensing. *ACS Appl. Nano Mater.* **2020**, *3* (5), 4788−4798.
(53) Liu, X.; Long, L.; Yang, W.; Chen, L.; Jia, J. Facilely Electrodeposited Coral-like Copper Micro-/Nano-Structure Arrays with Excellent Performance in Glucose Sensing. *Sensors Actuators, B Chem.* **2018**, *266*, 853−860.
(54) Jiménez-Fiérrez, F.; González-Sánchez, M. I.; Jiménez-Pérez, R.; Iniesta, J.; Valero, E. Glucose Biosensor Based on Disposable Activated Carbon Electrodes Modified with Platinum Nanoparticles Electrodeposited on Poly(Azure A). *Sensors* **2020**, *20* (16), 1−15.
(55) Fatoni, A.; Widanarto, W.; Anggraeni, M. D.; Dwiasi, D. W. Glucose Biosensor Based on Activated Carbon − $NiFe_2O_4$ Nanoparticles Composite Modified Carbon Paste Electrode. *Results Chem.* **2022**, *4* (May), No. 100433.
(56) Arikan, K.; Burhan, H.; Sahin, E.; Sen, F. A Sensitive, Fast, Selective, and Reusable Enzyme-Free Glucose Sensor Based on Monodisperse AuNi Alloy Nanoparticles on Activated Carbon Support. *Chemosphere* **2022**, *291* (March), No. 132718.
(57) Hossain, M. F.; Park, J. Y. Plain to Point Network Reduced Graphene Oxide-Activated Carbon Composites Decorated with Platinum Nanoparticles for Urine Glucose Detection. *Sci. Rep.* **2016**, *6* (February), 1−10.
(58) Saravanan, J.; Pannipara, M.; Al-Sehemi, A. G.; Talebi, S.; Periasamy, V.; Shah, S. S.; Aziz, M. A.; Gnana kumar, G. Flower-like CuO/NiO Nanostructures Decorated Activated Carbon Nanofiber Membranes for Flexible, Sensitive, and Selective Enzyme-Free Glucose Detection. *J. Mater. Sci. Mater. Electron.* **2021**, *32* (20), 24775−24789.
(59) Kumar, V.; Shukla, S. K.; Choudhary, M.; Gupta, J.; Chaudhary, P.; Srivastava, S.; Kumar, M.; Kumar, M.; Sarma, D. K.; Yadav, B. C.; Verma, V. Ti_2C-TiO_2 MXene Nanocomposite-Based High-Efficiency Non-Enzymatic Glucose Sensing Platform for Diabetes Monitoring. *Sensors* **2022**, *22* (15), 1−11.
(60) Huang, Y.; Long, Z.; Zou, J.; Luo, L.; Zhou, X.; Liu, H.; He, W.; Shen, K.; Wu, J. A Glucose Sensor Based on Surface Functionalized MXene. *IEEE Trans. Nanotechnol.* **2022**, *21*, 399−405.
(61) Kulkarni, T.; Slaughter, G. Application of Semipermeable Membranes in Glucose Biosensing. *Membranes (Basel).* **2016**, *6* (4). DOI: 10.3390/membranes6040055.

https://doi.org/10.1021/acsomega.3c09659
ACS Omega XXXX, XXX, XXX−XXX